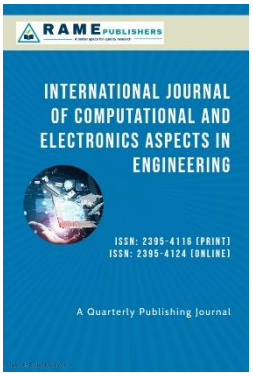
International Journal of Computational and Electronics Aspects in Engineering
Volume 7, Issue 5, November 2026, pp 659 - 672
https://doi.org/10.26706/ijceae.7.5.20261010

Outage-Aware Smart Charging of Electric Vehicles in Weak Distribution Grids: Reinforcement Learning versus Model-Predictive Control

Mohammed Tariq Majeed*

Department of Medical Instrumentation Techniques Engineering, Polytechnic College Mosul, Northern Technical University, Mosul, Iraq.

Correspondence: aldabgh68@ntu.edu.iq



Article – Peer Reviewed
Received: 30 August 2026
Accepted: 28 October 2026
Published: 10 November 2026

Copyright: © 2026 RAME Publishers
This is an open access article under the CC BY 4.0 International License.

https://creativecommons.org/licenses/by/4.0/

Cite this article: Mohammed Tariq Majeed, "Outage-Aware Smart Charging of Electric Vehicles in Weak Distribution Grids: Reinforcement Learning versus Model-Predictive Control", *International Journal of Computational and Electronics Aspects in Engineering*, RAME Publishers, vol. 7, issue 5, pp. 659-672, 2026.
https://doi.org/10.26706/ijceae.20261010

Abstract: Charging electric vehicles in weak distribution grids with rationed electricity supply requires a controller that respects voltage and transformer limits, anticipates supply interruptions and decides when to use costly backup generation. This study compared reinforcement learning with model-predictive control for this task. A car park with 24 chargers at the end of a rural low-voltage benchmark feeder was simulated with 9148 real charging sessions and household load profiles, under rotating outage schedules of 20, 16 and 12 hours of daily supply that included schedule deviations and unscheduled interruptions. Uncontrolled charging, least-laxity-first rules with and without outage awareness, rolling-horizon model-predictive control, three proximal-policy-optimisation agents and a perfect-information benchmark were evaluated on 122 held-out days, and all schedules were checked with alternating-current power flow. Uncontrolled charging violated the 0.90 per-unit voltage limit in 6.4% of charging intervals and overloaded the transformer by up to 35%, whereas all controlled strategies remained within the limits. Outage awareness reduced the unmet energy by 4–22%, and the reduction grew with outage severity. A simple outage-aware least-laxity rule matched model-predictive control to within 0.2% in daily cost. The learning agents lowered the daily cost by 1–5% by rationing generator energy more cautiously, but their advantage varied between training seeds, vanished when schedule information was missing and reversed when true departure times were available. Departure-time uncertainty, rather than outage uncertainty, explained 87% of the cost gap to perfect information.

Keywords: electric vehicle smart charging; reinforcement learning; model-predictive control; power outages; load shedding; weak distribution grid; voltage constraints; backup generator

1. Introduction

Electric vehicles (EVs) shift a large part of transport energy demand onto distribution networks that were not designed for it. Even in well-supplied grids, unmanaged charging raises local peaks, depresses voltages at the ends of long feeders and overloads distribution transformers [1, 2]. Smart charging, which adjusts when and how fast each vehicle charges, is the standard remedy. A large body of work has developed optimisation-based and learning-based controllers for this task [2, 3]. Artificial-intelligence methods, from neural networks to predictive energy management, are also used increasingly in power systems with a high share of renewable generation [4, 5].

Many electricity systems face a further difficulty: the grid is not always there. In Iraq, generation has lagged far behind demand for two decades. Households experience daily interruptions of the public supply that commonly last 8–18 hours, and they rely on neighbourhood diesel generators that sell a few amperes per household at a cost several times that of grid electricity [6, 7]. Supply is rationed by rotating schedules that are announced to consumers, but the realised outages deviate from these schedules, and unscheduled interruptions are frequent. Similar planned load shedding affects South Africa

and other developing economies [8]. Recent studies have begun to examine EV charging under such conditions. Yu et al. [9] planned parking-lot charging stations for periods of prolonged load shedding, and Einolander et al. [10] valued bidirectional EVs as a household backup during outages. The real-time control of EV charging in a grid that is both weak and intermittently unavailable, however, has received little attention.

Such a setting changes the charging problem in two ways. First, energy that is not delivered while the grid is available may never be delivered before the vehicle leaves. A controller must therefore look ahead to the next outage and decide which vehicles to serve first. Second, the backup supply, typically a diesel generator, is limited in capacity and expensive. Whether to buy generator energy during an outage, or to wait for the grid to return, depends on uncertain outage durations and departure times. Both decisions are made under the voltage and transformer limits of a weak feeder, and these limits leave less room for catching up after the grid returns. Weak feeders with converter-connected sources also suffer from power-quality problems, which storage and active filtering can reduce [11].

Two families of controllers are natural candidates. Model-predictive control (MPC) solves a finite-horizon optimisation problem at each step with forecasts of arrivals, departures and grid conditions, applies the first decision and repeats [12, 13]. MPC handles constraints explicitly, but it depends on forecasts and on solving an optimisation problem online. Deep reinforcement learning (RL) learns a policy from simulated experience and can be evaluated in microseconds. It has been applied to charging stations [14], homes [15], residential microgrids with safety layers [16] and networks with voltage constraints [17]. RL can, in principle, learn to anticipate uncertain events from their statistics, but it offers no guarantees and is sensitive to its training distribution [3]. Comparisons of the two families in other domains suggest that each has advantages [18], yet a direct, controlled comparison for EV charging under grid outages is missing. Such a comparison should use the same data, constraints and information for both families, together with simple heuristic baselines and a perfect-information bound.

This paper provides that comparison. The setting is a 24-charger car park at the end of a weak rural low-voltage feeder whose supply follows rotating outage schedules. The contributions are as follows:

1. A reproducible benchmark that combines real charging sessions (ACN-Data, Caltech) [19], a public low-voltage benchmark network with household load profiles (SimBench) [20], and an outage model parameterised from reported Iraqi supply patterns. The benchmark includes realistic forecast errors: deviations from the announced schedule, unscheduled outages and departure-time uncertainty.
2. An outage-aware formulation of charging control with a backup generator, together with an outage-aware least-laxity-first heuristic that requires no optimisation.
3. A controlled comparison of uncontrolled charging, two heuristics, rolling-horizon MPC, a proximal-policy-optimisation (PPO) agent and a perfect-information optimum. The comparison covers three outage severities and is evaluated on held-out days, with all grid constraints checked by AC power flow.
4. An analysis of the value of outage information and departure forecasts, and of the computational cost of each controller.

The remainder of the paper is organised as follows. Sections 1.1–1.3 review related work. Section 2 describes the system model, the data and the controllers. Section 3 presents and discusses the results, and Section 4 concludes.

1.1. Optimisation-based and model-predictive charging control

Optimisation-based scheduling of EV charging ranges from day-ahead robust scheduling of charging stations under price and load uncertainty [13] to stochastic MPC of fast-charging hubs with uncertain demand [12]. Online scheduling rules with performance guarantees, such as least-laxity-first and its smoothed variant, have been analysed theoretically [21], and the open session data of the Caltech Adaptive Charging Network support their evaluation [19]. Reviews identify MPC as the dominant real-time method in charging-station operation, because it handles network limits and user requirements explicitly [2]. Its weaknesses are its reliance on forecasts and the cost of online optimisation.

1.2. Reinforcement learning for EV charging

RL has been applied to EV charging at many scales [3]. Li et al. [14] used multi-agent deep RL to control the power of each charger at a station in real time. Mansour et al. [15] combined a soft actor-critic agent for EV charging with a mixed-integer programme for a smart home. Zhang et al. [16] grouped vehicles and used constrained RL with a safety filter in a residential microgrid. Liu et al. [17] coordinated EV charging with voltage-control devices on a 33-bus network. Common issues are safety during operation, the size of the action space when each charger is controlled separately, and

generalisation beyond the training conditions [3]. A common remedy, adopted here, is to let the agent choose an aggregate set-point and to dispatch it to vehicles with a priority rule inside a safety layer.

1.3. Charging under grid outages

Most smart-charging studies assume a permanently available grid. Planned load shedding has been studied mainly from the perspectives of consumers [8] and infrastructure planning [9], and EVs have been studied as backup sources for households [10]. In Iraq, the neighbourhood-generator economy shows the scale of the problem. Generator electricity costs more than ten times the grid tariff, and households typically buy less than 10 A of generator supply [6]. To the author's knowledge, no study has compared learning-based and optimisation-based real-time charging control under scheduled and unscheduled outages in a voltage-constrained feeder.

2. Materials and Methods

Figure 1 summarises the studied system. A car park with 24 chargers is supplied from the end of a weak rural low-voltage feeder. The medium-voltage supply follows a rotating outage schedule, and during outages the chargers can be supplied only by a small diesel generator. A controller decides every 15 minutes how much power each connected vehicle receives.

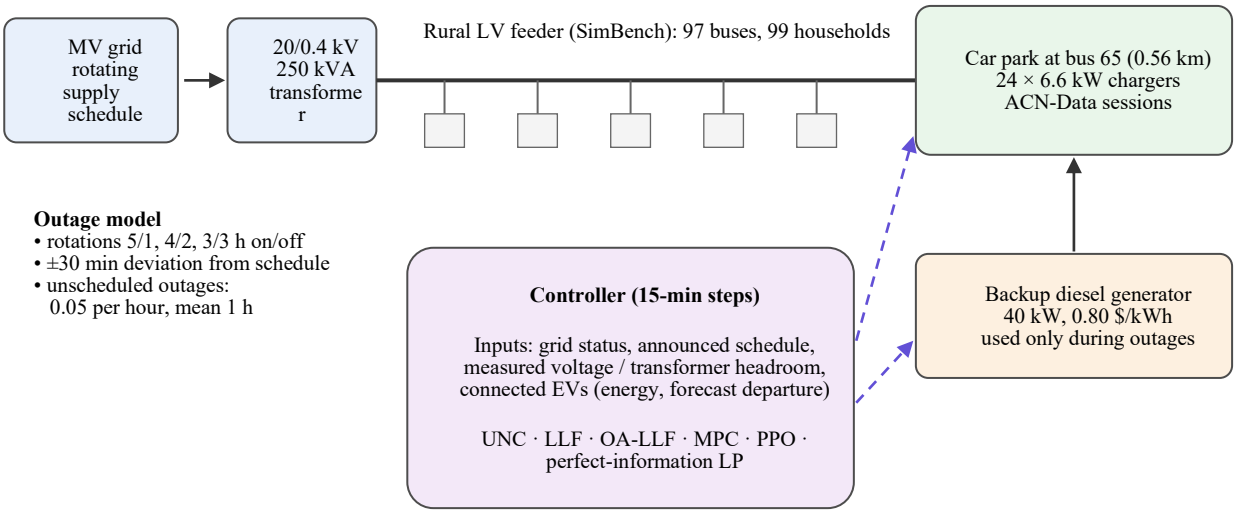


Figure 1. Overview of the studied system: a 24-charger car park at the end of a rural low-voltage feeder whose supply follows a rotating outage schedule, a backup diesel generator for outage periods, and the controllers compared in this study.

2.1. Distribution network and household demand

The network is the SimBench rural low-voltage benchmark grid 1-LV-rural2 [20]. It has a 20/0.4 kV, 250 kVA transformer (v_k = 6%), 97 buses, 1.47 km of NAYY 4×150 cables and 99 household connections with standard 15-minute load profiles for a full year. Two modifications represent a weak grid in a hot climate. First, the household active and reactive profiles were scaled by a factor of 2, because Iraqi households consume far more electricity than the Central European households of the benchmark; a typical Iraqi household uses about 1,740 kWh in a summer month [6]. Second, the rooftop photovoltaic units of the benchmark were disconnected. The car park was connected to bus 65, the electrically most remote bus, 0.56 km from the transformer. All power flows were computed with pandapower [22].

Running AC power flows inside every controller would be too slow for a fair comparison. Instead, for each 15-minute interval of the year, two AC power flows were solved: one with the household demand only, and one with an additional 100 kW at the car park. From these, the minimum bus voltage V_t^0, the transformer apparent power S_t^0 and their sensitivities to the car-park power, σ_t^V (pu per kW) and σ_t^S (kVA per kW), were obtained. The resulting charging headroom is

$$H_t = \max\left\{0, \min\left(\frac{V_t^0 - V_{\text{lim}}}{\sigma_t^V}, \frac{S_{\text{rated}} - S_t^0}{\sigma_t^S}\right)\right\} \quad (1)$$

where V_{lim} = 0.91 pu is the controller's voltage target. The target is 0.01 pu above the 0.90 pu limit of EN 50160 [23], to absorb linearisation error. The headroom ranged from 93 to 128 kW (1st to 95th percentile), which is less than the 158 kW

that all 24 chargers draw together. The network constraint is therefore active whenever many vehicles charge at once. Controllers observe the actual headroom of the current interval, as a voltage measurement at the car park would provide. For future intervals they use the headroom computed from the household demand of the same weekday one week earlier, which serves as the load forecast.

2.2. Charging sessions

Charging sessions were taken from ACN-Data, the open dataset of the Caltech Adaptive Charging Network [19]. The data were obtained in the processed form distributed with the evprof package. Only pre-pandemic weekdays between November 2018 and February 2020 were used. Sessions from 24 of the 52 Caltech chargers were selected at random (fixed seed) to obtain a car park of realistic size for a low-voltage feeder. Timestamps were converted to local time and discretised to 15-minute steps of an operating day running from 05:00 to 05:00. Each charger was given a maximum power of 6.6 kW. The energy demand of a session was set to the energy actually delivered in the data, capped at what 6.6 kW could deliver during the connection. The resulting set has 9148 sessions on 333 days. The training period is November 2018 to August 2019 (211 days), and the held-out test period is September 2019 to February 2020 (122 days). Over all 333 days, an average of 27.5 vehicles arrived per day, mainly between 06:00 and 09:00, stayed 7.5 h and requested 416 kWh in total. The corresponding values for the test days are given in Table 1.

The controllers know the energy request of a vehicle at arrival but not its departure time. Departure was forecast as the arrival time plus the median connection duration of the same user in the training period, or the overall median for new users. On the test days this forecast had a mean absolute error of 1.92 h, and half of the vehicles left before their forecast departure. A conservative variant used the user's 25th-percentile duration instead.

Table 1. Characteristics of the test case.

Item	Value
Network	SimBench 1-LV-rural2: 20/0.4 kV, 250 kVA transformer, 97 buses, 99 households, 1.47 km cable
Household demand	SimBench standard profiles (15 min, one year), scaled × 2; PV disconnected
Car park	24 chargers × 6.6 kW (158 kW total) at bus 65, 0.56 km from the transformer
Charging sessions	ACN-Data (Caltech), weekdays Nov 2018–Feb 2020: 5730 training sessions (211 days), 3418 test sessions (122 days)
Test-day statistics	28.0 sessions/day; 438 kWh/day; mean stay 7.3 h
Departure forecast	user median stay (training period); mean absolute error 1.92 h on test days
Outage severities	S20 (5 h on/1 h off), S16 (4/2), S12 (3/3); ±30 min deviation; unscheduled outages 0.05 h^{-1}, mean 1 h
Backup supply	40 kW diesel generator, available only during outages
Prices	grid 0.05 \$/kWh; generator 0.80 \$/kWh; unmet energy 1.50 \$/kWh
Limits	voltage ≥ 0.90 pu (controller target 0.91 pu); transformer ≤ 250 kVA

2.3. Outage model

The supply follows a rotating schedule with fixed on and off blocks. This reflects the rationing practice of Iraqi distribution companies, which leaves households with roughly 6–16 h of public supply per day in summer [6, 7]. Three severities were studied: S20 (5 h on, 1 h off), S16 (4 h on, 2 h off) and S12 (3 h on, 3 h off). The phase of the rotation was drawn at random for each day, and the schedule was announced to the controllers before the day began. The realised outages differ from the announced schedule in two ways. The start and end of each scheduled outage were shifted independently by up to ±30 min (uniform, in 15-minute steps). In addition, unscheduled outages start at a rate of 0.05 per hour of supply, with a geometrically distributed duration of mean 1 h. Two outage realisations (seeds) were generated for every test day and severity, and all controllers faced the same realisations. During an outage the whole feeder is de-energised, and the car park can draw only on a 40 kW diesel generator.

2.4. Objective

The operating cost of a day is

$$J = \sum_t \left(c_{\mathrm{g}} P_t^{\mathrm{grid}} + c_{\mathrm{d}} P_t^{\mathrm{gen}} \right) \Delta t + c_{\mathrm{u}} \sum_i E_i^{\mathrm{unmet}} \tag{2}$$

where Δt = 0.25 h and E_i^{unmet} is the energy still missing when vehicle i actually departs. The prices are c_{g} = 0.05 \$/kWh for grid energy and c_{d} = 0.80 \$/kWh for generator energy, which lies within the range of levelised costs reported for Iraqi

neighbourhood generators [6]. Unmet energy is penalised at c_{u} = 1.50 \$/kWh. The penalty exceeds the generator cost, so a controller should use the generator when it is the only way to serve a vehicle before it leaves. The network limits (voltage ≥ 0.90 pu at every bus, transformer loading ≤ 100%) are treated as constraints, and their violations are reported separately.

2.5. Controllers

Six controllers were compared. All except the uncontrolled case and the perfect-information benchmark see the same information: the grid status, the announced schedule, the measured and forecast headroom, and the energy and forecast departure of each connected vehicle.

- **Uncontrolled (UNC).** Every connected vehicle charges at 6.6 kW whenever the grid is available. The chargers stop during outages, and network limits are ignored.
- **Least-laxity first (LLF).** The aggregate grid power equals the measured headroom. It is dispatched to vehicles in order of increasing laxity, $\ell_i = (d_i - k)\Delta t - E_i/P_{\max}$, where d_i is the forecast departure step and E_i the remaining energy [21]. During an outage, the generator serves only vehicles whose remaining energy cannot be delivered at full power before their forecast departure. In this calculation the controller assumes that the grid returns at the next step. LLF is therefore network-aware but outage-unaware.
- **Outage-aware LLF (OA-LLF).** The same rule, but laxity and generator need are computed from the number of grid-available steps before departure according to the announced schedule. Vehicles that will lose supply during an upcoming outage thus move up the priority list, and the generator serves exactly the energy that the scheduled grid supply cannot deliver.
- **Model-predictive control (MPC).** At every step, a linear programme is solved over the rest of the operating day. Its variables are the grid and generator power of each vehicle in each step and its unmet energy. It minimises Eq. (2) subject to per-vehicle power limits, energy balances, the headroom forecast and the announced schedule, with a negligible penalty on delay to favour early charging. Only the first step is applied. The LP is solved with HiGHS [24] through SciPy.
- **Reinforcement learning (PPO).** A proximal-policy-optimisation agent [25] chooses two continuous actions every step: the aggregate grid power as a fraction of the measured headroom, and the generator power as a fraction of its rating. The power is dispatched in OA-LLF order, so the agent cannot exceed the headroom or the generator rating. Its 14 observations describe the time of day, the grid status, the announced time to the next outage and its length, the remaining outage time, and aggregate vehicle states: the number connected, the total remaining energy, the energy that the scheduled supply cannot deliver, the energy of vehicles due to leave within 2 h, and the minimum and median outage-aware laxity. They also include the current and forecast headroom. The reward is the negative of the cost terms of Eq. (2) incurred in each step. The agent was trained with Stable-Baselines3 [26] on the 211 training days, with severity and outage realisation drawn at random for every episode. Training used 1.5 million steps, 4 parallel environments, a 64-64 network, γ = 0.995 and default PPO settings otherwise. Three agents with different random seeds were trained and are reported separately.
- **Perfect information (PI).** A single LP per day with the true arrivals, departures, outages and headroom. It gives a lower bound on the achievable cost.

2.6. Evaluation

All controllers were evaluated on the 122 test days for each severity and both outage seeds, that is, 244 simulated days per severity. The metrics were the share of requested energy not delivered by departure, the number of vehicles that left with more than 1 kWh missing, generator energy, daily cost, and network-limit violations. The schedules of all controllers were checked with full AC power flows for severity S16 (seed 0). Additional experiments for severity S16 measured the value of information: exact outage schedules, no schedule information, true departure times, and the conservative departure forecast.

3. Results and Discussion

3.1. Test case

Figure 2 characterises the test case. Vehicles arrived mainly between 06:00 and 09:00 and left between 15:00 and 19:00. Most requested less than 20 kWh, but a long tail asked for up to 60 kWh. The charging headroom of the feeder fell to about 105 kW during working hours and recovered to about 125 kW at night. This is well below the 158 kW that the car park can

draw. The realised supply averaged 19.1, 15.3 and 11.6 h per day in the three severities. These values are below the nominal 20, 16 and 12 h because of the unscheduled outages.

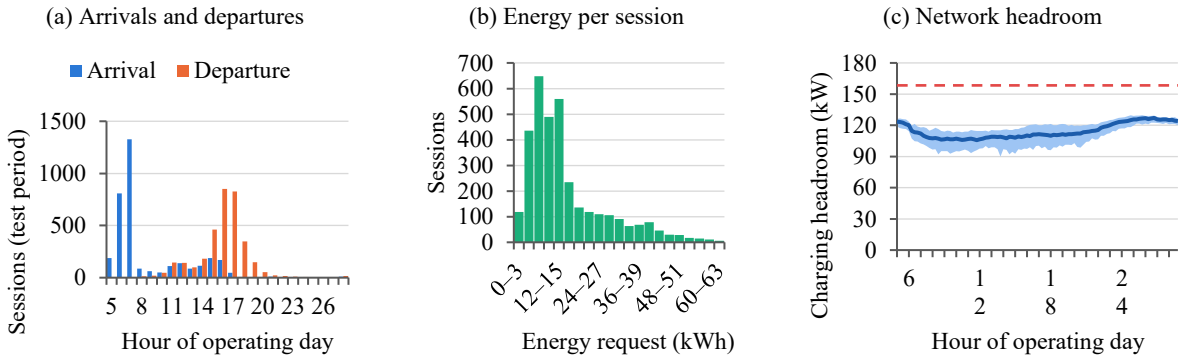
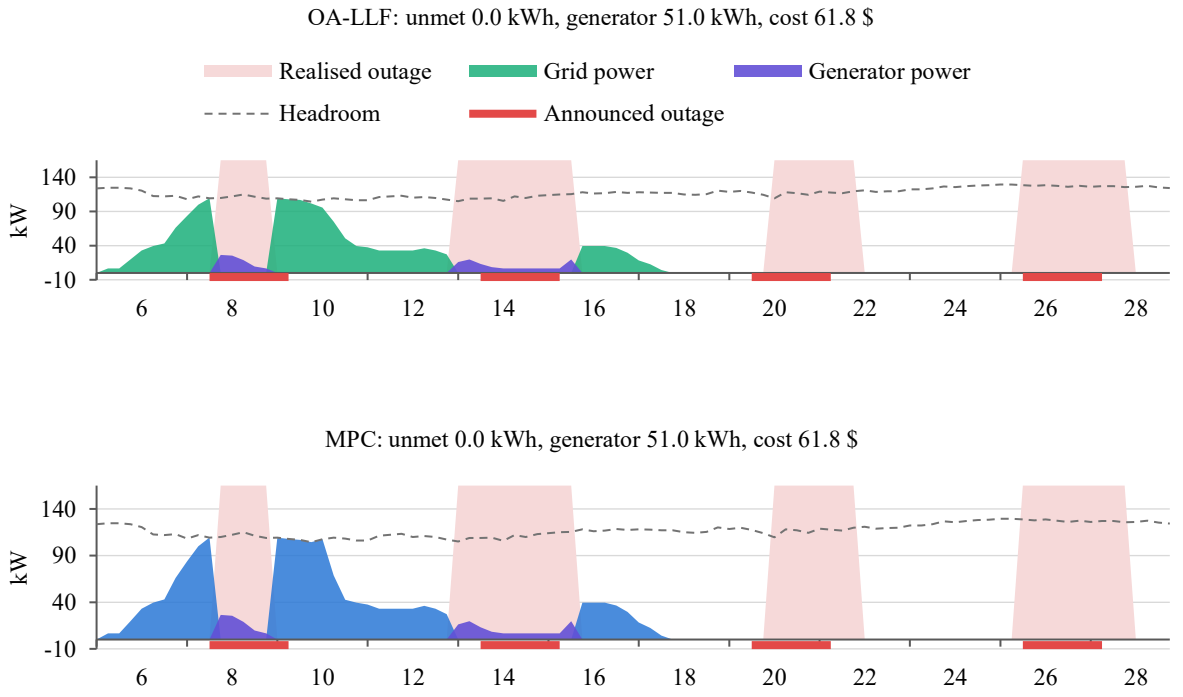


Figure 2. Test case. (a) Arrival and departure times of the 3418 test-period sessions; (b) energy requested per session; (c) charging headroom at the car-park bus over the operating day (test days; line: median, shaded band: 5th–95th percentile), compared with the total rating of the 24 chargers (dashed line).

Figure 3 shows a typical test day under severity S16 (30 sessions, 471 kWh requested). The announced outages (red bars) and the realised ones (shading) differ by up to 30 minutes. The grid power of every network-aware controller stays below the headroom. OA-LLF and MPC produced identical schedules. Both served the vehicles that would otherwise leave unserved from the generator during the morning and afternoon outages, using 51 kWh of generator energy. The PPO agent used half as much generator energy (26 kWh), accepted 10 kWh of unmet demand and achieved a lower cost. The perfect-information benchmark needed the same 26 kWh of generator energy as PPO but left no vehicle unserved, because it knew which vehicles would actually stay until the grid returned.



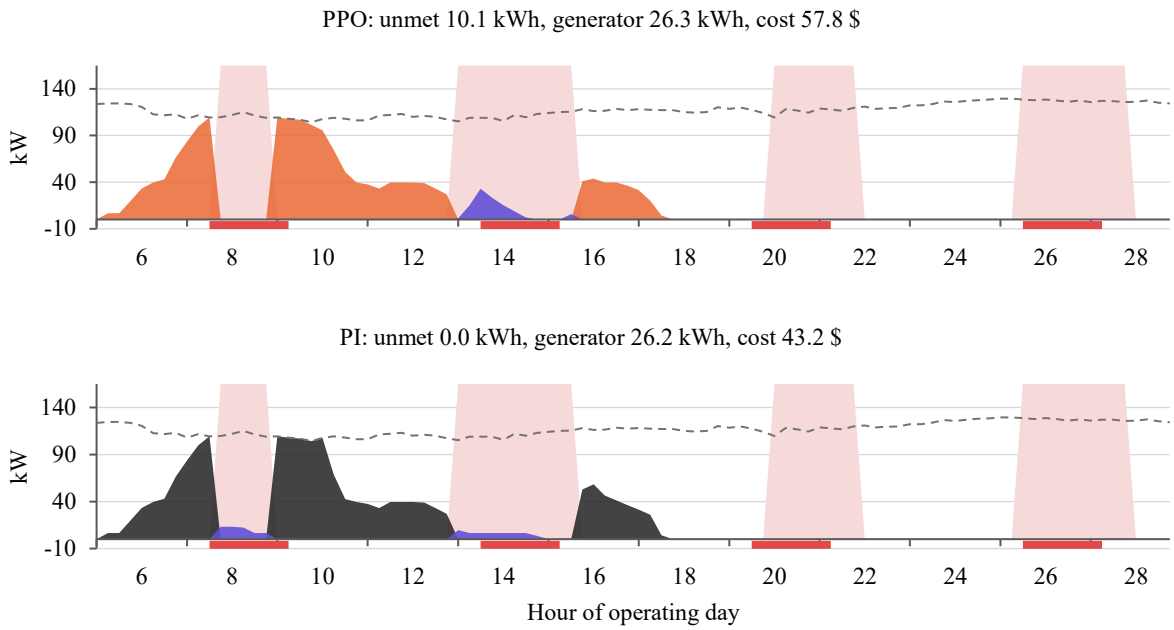


Figure 3. Charging schedules on a typical test day (11 September 2019, severity S16, outage seed 0) for OA-LLF, MPC, PPO (seed 0) and the perfect-information benchmark. Coloured areas are grid power, purple areas are generator power, the dashed line is the network headroom, shading marks realised outages and red bars mark announced outages.

3.2. Comparison of controllers

Table 2 and Figure 4 summarise the 244 simulated test days of each severity. Uncontrolled charging left 3.4%, 9.2% and 18.9% of the requested energy undelivered in S20, S16 and S12, because its chargers stop during every outage. It also violated the network limits. Under S16, the AC power flow found the minimum voltage below 0.90 pu in 278 of 4331 charging intervals (6.4%), with a lowest value of 0.832 pu. The transformer was overloaded in 122 intervals, by up to 35%.

All network-aware controllers kept the voltage and the transformer loading within limits in every interval. The outage-unaware LLF already removed 40–55% of the unmet energy of uncontrolled charging. Making the rule outage-aware (OA-LLF) reduced the unmet energy further, by 4%, 14% and 22% in S20, S16 and S12, at the price of more generator energy. The benefit therefore grows with outage severity. MPC performed almost identically to OA-LLF in every severity: daily costs within 0.2%, and unmet energy within 0.02 percentage points. With a single binding network limit and linear costs, prioritising vehicles by outage-aware laxity is close to what a rolling-horizon optimisation with the same forecasts does.

Table 2. Results on the held-out test days (122 days × 2 outage realisations per severity). Unmet energy is relative to the total energy requested; "short" counts vehicles leaving with more than 1 kWh missing. PPO values are the mean of three agents with the range in brackets. Violations are counted with the linear network model; AC results are given in Section 3.4.

Severity (supply h/day)	Controller	Unmet energy (%)	Vehicles short per day	Generator (kWh/day)	Cost ($/day)	Voltage / overload violations (intervals)
S20 (19.1)	UNC	3.36	2.65	0.0	43.19	404 / 105
S20 (19.1)	LLF	2.02	2.03	12.1	43.75	0 / 0
S20 (19.1)	OA-LLF	1.93	1.93	13.3	44.08	0 / 0
S20 (19.1)	MPC	1.94	1.95	13.3	44.14	0 / 0
S20 (19.1)	PPO	2.50 [2.17–2.67]	2.20 [1.96–2.36]	5.7 [4.2–7.7]	41.97 [41.46–42.46]	0 / 0
S20 (19.1)	PI	0.00	0.00	14.7	32.91	0 / 0
S16 (15.3)	UNC	9.18	5.40	0.0	80.14	531 / 182
S16 (15.3)	LLF	4.81	3.81	30.3	75.16	0 / 0
S16 (15.3)	OA-LLF	4.13	3.37	35.2	74.50	0 / 0
S16 (15.3)	MPC	4.15	3.45	35.3	74.65	0 / 0

Severity (supply h/day)	Controller	Unmet energy (%)	Vehicles short per day	Generator (kWh/day)	Cost ($/day)	Voltage / overload violations (intervals)
S16 (15.3)	PPO	5.31 [4.90–5.82]	3.79 [3.62–3.93]	22.3 [19.6–25.1]	72.34 [71.75–73.49]	0 / 0
S16 (15.3)	PI	0.00	0.00	40.2	52.02	0 / 0
S12 (11.6)	UNC	18.89	8.48	0.0	141.81	647 / 244
S12 (11.6)	LLF	8.43	5.88	60.3	120.65	0 / 0
S12 (11.6)	OA-LLF	6.59	4.81	71.9	117.67	0 / 0
S12 (11.6)	MPC	6.58	4.88	72.3	117.88	0 / 0
S12 (11.6)	PPO	8.12 [7.05–9.27]	5.37 [5.05–5.75]	57.0 [50.3–62.8]	116.23 [113.73–118.46]	0 / 0
S12 (11.6)	PI	0.00	0.00	83.0	84.18	0 / 0

The PPO agents achieved the lowest daily cost of all implementable controllers in every severity. On average they were cheaper than MPC by 4.9% in S20, 3.1% in S16 and 1.4% in S12 (Table 3). The advantage was significant for all three agents in S20 (paired bootstrap over test days), for two of three in S16 and for one of three in S12. The agents did not achieve this by delivering more energy. On the contrary, they left slightly more energy undelivered than MPC (2.5%, 5.3% and 8.1% against 1.9%, 4.1% and 6.6%). Instead, they bought 21–57% less generator energy. In other words, PPO found a different trade-off between the two costly resources, generator energy and unmet demand, than the forecast-driven controllers.

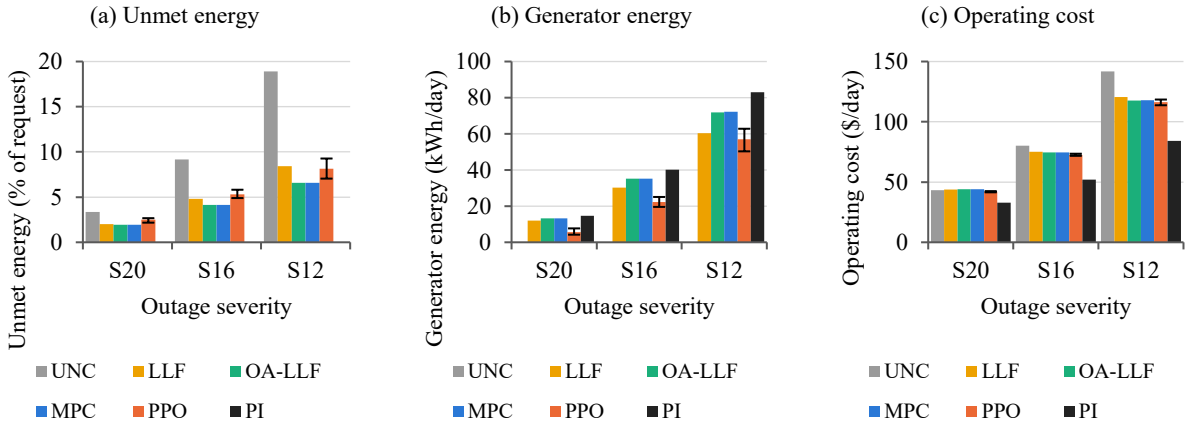


Figure 4. Unmet energy, generator energy and operating cost per controller and outage severity. Error bars on PPO show the range over three training seeds. The cost of UNC excludes its network-limit violations.

Table 3. Daily cost difference of the PPO agents relative to MPC: mean difference in $/day with the 95% bootstrap confidence interval over test days, and relative difference.

Severity	PPO seed 0	PPO seed 1	PPO seed 2	Mean of agents
S20	**−2.14 [−2.93, −1.30]; −4.9%**	**−1.68 [−2.59, −0.76]; −3.8%**	**−2.68 [−3.49, −1.84]; −6.1%**	**−2.17 [−2.98, −1.37]; −4.9%**
S16	**−2.90 [−4.11, −1.76]; −3.9%**	−1.16 [−2.76, +0.58]; −1.6%	**−2.88 [−4.09, −1.71]; −3.9%**	**−2.31 [−3.59, −1.00]; −3.1%**
S12	**−4.15 [−5.72, −2.62]; −3.5%**	+0.58 [−1.35, +2.53]; +0.5%	−1.39 [−2.94, +0.27]; −1.2%	−1.65 [−3.33, +0.01]; −1.4%

Figure 5 tests whether this trade-off could also be obtained by tuning the forecast-driven controllers. The departure forecast of OA-LLF and MPC was varied from the 10th to the 75th percentile of each user's historical connection time. Earlier (more conservative) departure forecasts reduce unmet energy, but they buy generator energy for many vehicles that would have stayed long enough to be served by the grid. With the 10th percentile, unmet energy fell to 1.0%, but the cost

rose to 94 $/day. Later forecasts lowered the cost only to 74 $/day. Two of the three PPO agents lay clearly below this cost–unmet frontier, at 71.8 $/day with 4.9–5.2% unmet energy. The third lay on it. The learned policy therefore exploits structure that a single departure quantile cannot capture.

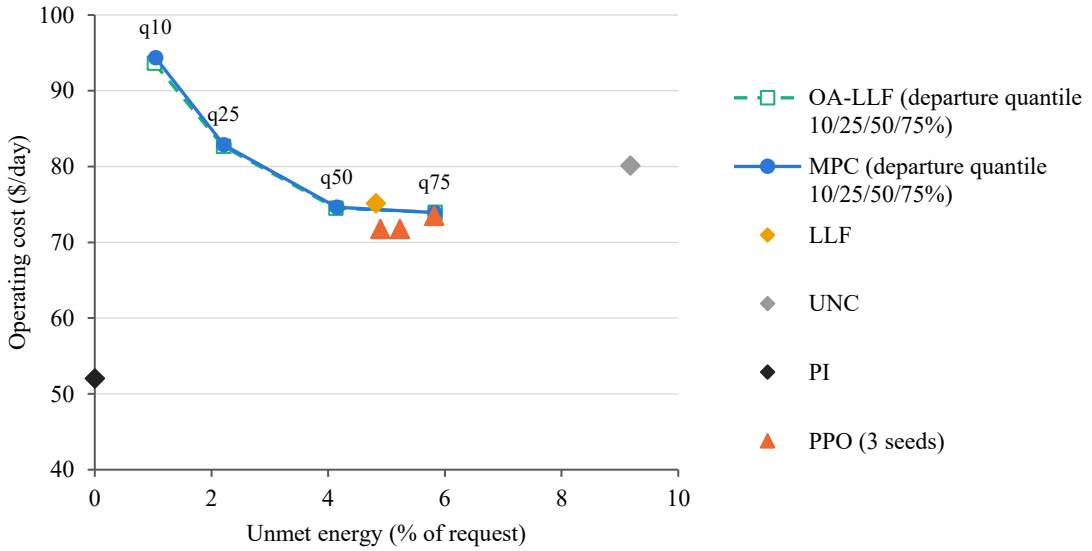


Figure 5. Operating cost against unmet energy under severity S16. OA-LLF and MPC are shown for departure forecasts at the 10th, 25th, 50th (base) and 75th percentile of each user's training-period connection time; the MPC points are labelled with the quantile.

Figure 6 shows how the agent spends generator energy. OA-LLF buys exactly the energy that the announced grid supply cannot deliver before the forecast departures, so its generator power grows in proportion to this shortfall. PPO responded much more weakly. It used only 4–8 kW whenever the computed shortfall exceeded 5 kWh, even when it exceeded 30 kWh. It also ran the generator at a low level (about 2.6 kW) when no shortfall was computed. Because half of the vehicles actually leave before their median-based forecast, and others stay longer, the computed shortfall is a noisy signal. The agent learned to hedge against this noise from experience on the training days.

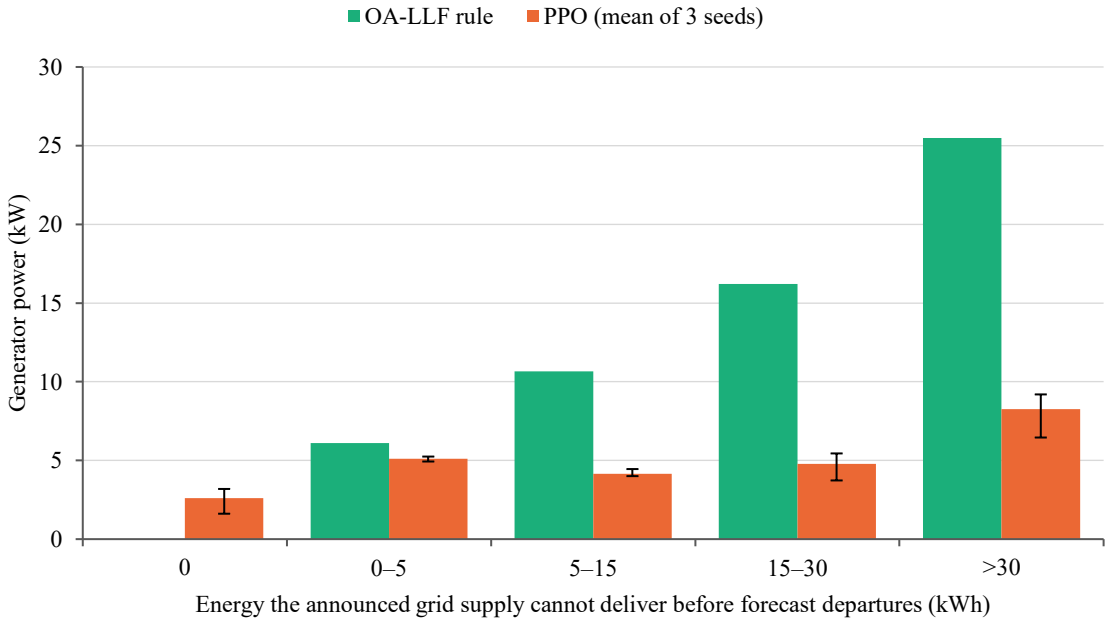


Figure 6. Mean generator power during outages (severity S16) as a function of the energy that the announced grid supply cannot deliver before the forecast departures of the connected vehicles. Error bars on PPO show the range over three seeds.

3.3. Value of information

Table 4 and Figure 7 compare the controllers under different information for severity S16. Without schedule information, OA-LLF and MPC fall back to outage-unaware behaviour, and their cost rose by only 0.8–0.9%. Under the base forecast errors, the announced schedule is therefore worth little to these controllers. The PPO agents, which had always seen the schedule during training, degraded much more without it. Their cost rose by 7–12%, and their generator use collapsed to 2–9 kWh/day, because the missing schedule features put them outside their training distribution. An exactly kept schedule without unscheduled outages reduced the cost of every controller by about 13% (MPC 74.7 to 64.9 $/day; PPO 72.3 to 62.7 $/day on average). Part of this reduction is due to the 0.7 h of extra daily supply.

The largest gain came from knowing departure times. With true departures, OA-LLF and MPC delivered virtually all requested energy (0.03% unmet) at 54.9 $/day, only 5.6% above the perfect-information cost of 52.0 $/day. Departure uncertainty thus accounts for 87% of the gap between MPC and perfect information. PPO, trained with forecast departures, improved only to 67.2–70.1 $/day. It could not exploit the better information as well as the optimisation-based controllers, and with true departures it was 22–28% more expensive than MPC.

Table 4. Value of information under severity S16: daily cost ($/day) and unmet energy (%) of OA-LLF, MPC and PPO (mean of three agents, range in brackets).

Information	OA-LLF cost (unmet %)	MPC cost (unmet %)	PPO cost (unmet %)
No schedule information	75.2 (4.81)	75.3 (4.82)	78.8 [77.2–80.2] (8.38)
Announced schedule (base)	74.5 (4.13)	74.7 (4.15)	72.3 [71.7–73.5] (5.31)
Exactly kept schedule	65.0 (3.71)	64.9 (3.69)	62.7 [62.3–63.4] (4.28)
True departure times	54.8 (0.03)	55.0 (0.03)	68.3 [67.2–70.1] (4.38)
Conservative departures (25th percentile)	82.7 (2.20)	82.9 (2.21)	–
Perfect information (PI)	52.0 (0.00)		

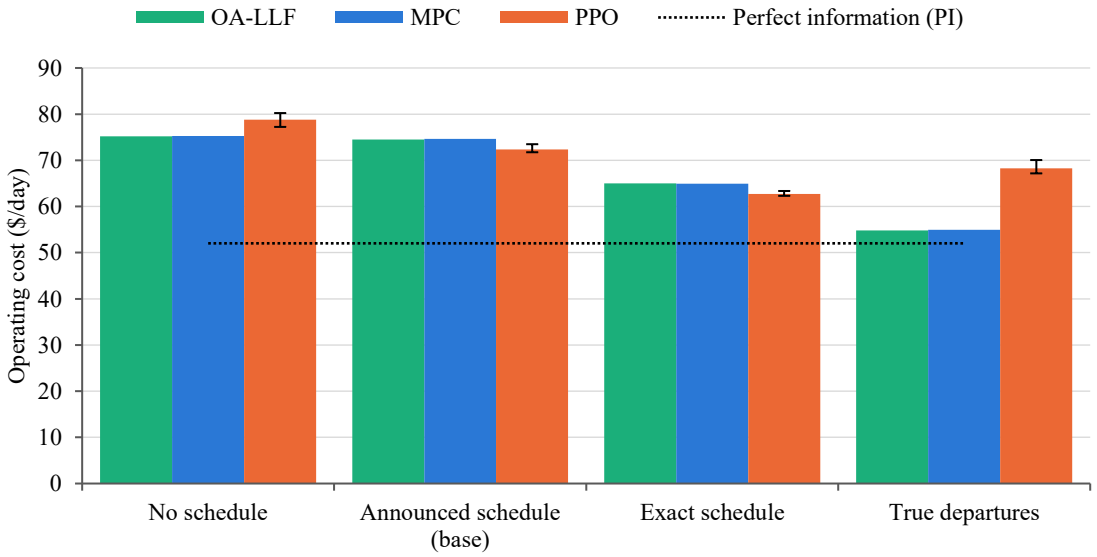


Figure 7. Daily cost of OA-LLF, MPC and PPO under severity S16 with no schedule information, the announced schedule (base case), an exactly kept schedule and true departure times. The dotted line is the perfect-information cost.

3.4. Network validation and computation

Figure 8 shows the AC power-flow check of all schedules for severity S16. Across 29,676 intervals with controlled charging, the lowest feeder voltage was 0.907 pu and the highest transformer loading 99.7%, so no network-aware controller violated a limit. The linearised headroom model of Eq. (1) differed from the AC power flow by 0.0016 pu on average (maximum 0.014 pu). It was conservative in the operating range near the voltage target, so the 0.01 pu margin was sufficient. Uncontrolled charging, in contrast, produced voltages down to 0.832 pu.

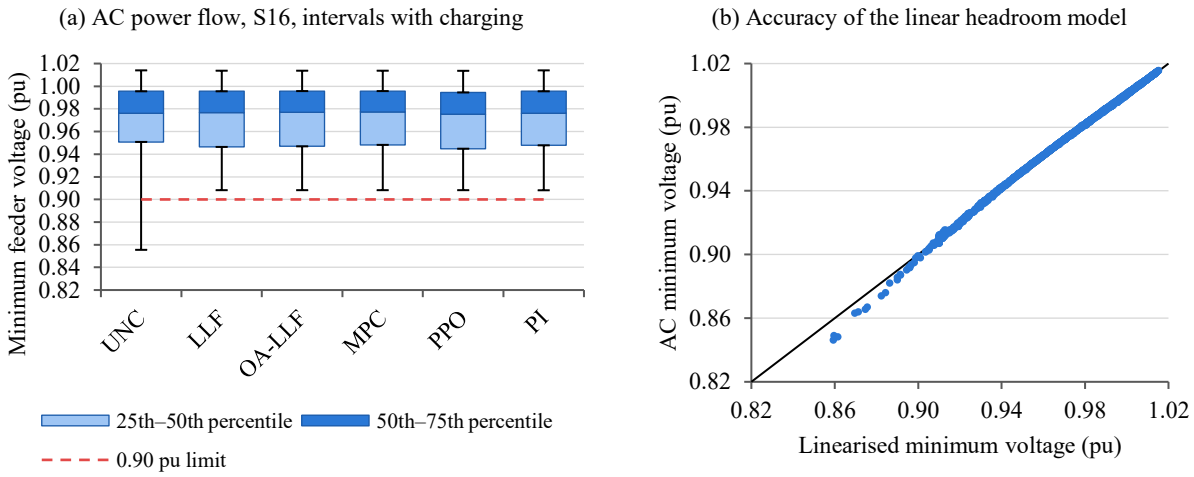


Figure 8. (a) Minimum feeder voltage from AC power flow in all intervals with charging (severity S16, outage seed 0, PPO pooled over three agents; boxes span the 25th–75th percentiles, whiskers the 0.5th–99.5th percentiles and the dashed line is the 0.90 pu limit); (b) linearised against AC minimum voltage for a random sample of these intervals.

Both controller families are computationally light at this scale. For severity S16, HiGHS solved the MPC linear programme in 4.0 ms on average and 26 ms at most on a single core. The PPO agent needed 0.4 ms per decision, including feature computation and dispatch. Training one agent took 11–12 min (1.5 million steps) on one CPU core.

3.5. Reinforcement learning versus model-predictive control

The title question has a nuanced answer. Under realistic forecast errors, the PPO agents reached a slightly lower operating cost than MPC (1–5% depending on outage severity), and two of three agents lay below the cost–unmet frontier that MPC and OA-LLF trace when their departure forecast is tuned (Figure 5). The source of this advantage is not better anticipation of outages. The agents used the generator less than the forecast-driven controllers, accepted somewhat more unmet energy, and rationed generator power in a way that reflects the noisiness of the departure forecasts (Figure 6). In effect, the agents learned a stochastic policy for a problem that MPC treats as deterministic. This agrees with the view that RL is most useful when uncertainty is hard to model explicitly [3].

The comparison also shows the costs of learning. The agents' performance varied between training seeds. Their advantage over MPC was statistically clear for all three agents only in the mildest severity. They failed badly when an input they had relied on during training (the announced schedule) was missing, and they could not exploit better information (true departure times) when it became available. MPC, in contrast, degraded gracefully without the schedule and improved by 26% with true departures, approaching the perfect-information cost within 6%. In practice, this means that MPC remains the safer choice when forecasts may improve over time or when inputs may fail, whereas an RL agent must be retrained whenever the information structure changes. Hybrid schemes that let RL tune the uncertainty handling of an MPC, as proposed for buildings [18], are a promising middle ground.

3.6. Simple rules capture most of the benefit

A practically important result is that the outage-aware least-laxity rule matched MPC almost exactly in every severity. The rule needs no solver, no load forecast beyond the current headroom and only the announced schedule. It can therefore run on the embedded controller of an existing charging station. Its advantage over the outage-unaware LLF grew with the severity of the outages, reaching 22% less unmet energy at 12 h of daily supply. For operators in grids with rationed supply, such as those in Iraq, this makes outage-aware prioritisation a low-cost first step. Optimisation and learning become worthwhile mainly once better departure information is available, for example from user inputs or booking systems.

3.7. Departure information matters more than outage information

Under the outage model used here, which includes ±30-minute schedule deviations and unscheduled outages, the announced schedule was worth less than 1% of the daily cost to OA-LLF and MPC. Knowing the true departure times was worth 26%. Outages make it necessary to buy expensive generator energy, but how much of that energy is really needed depends almost entirely on when the vehicles will leave. Collecting departure times from users, as the Caltech network does through its mobile application [19], is therefore the most valuable improvement for outage-prone car parks, more valuable than more accurate outage schedules. Exactly kept schedules would still be worth about 13% of the cost, which

shows the value of reliable rotation programmes for utilities. The required information can be collected with low-cost IoT hardware: ESP32-based nodes have been used for real-time fault monitoring of overhead power lines [27] and for energy monitoring and optimisation in buildings [28, 29], and lightweight protocols and encryption schemes are available to protect the data that such nodes exchange [30, 31].

3.8. Limitations

The results should be read with several limitations in mind. First, the charging sessions come from a Californian workplace car park, and the household profiles from a German benchmark scaled to a hotter climate. The outage process was parameterised from reported Iraqi supply hours rather than from measured outage logs, so absolute costs are illustrative. The relative ranking of the controllers, however, was largely consistent across the three severities. Second, the network was represented by a single binding headroom at the car-park bus. Settings with several interacting constraints, for example phase imbalance or multiple car parks, would favour MPC, which handles such constraints directly. Third, the agent was trained on one feeder and one car park, and its transfer to other sites was not tested. Fourth, battery ageing, generator start-up costs, emissions and user-specified priorities were not modelled. Finally, the prices used for grid, generator and unmet energy determine the trade-off that each controller makes. A different value of unmet demand would move all controllers along the frontier of Figure 5, but the dominance of the perfect-information solution and the importance of departure information would remain.

4. Conclusions

This paper compared rolling-horizon model-predictive control and deep reinforcement learning for charging electric vehicles at a car park on a weak rural feeder with rotating, imperfectly announced supply outages and a backup diesel generator. The comparison used real charging sessions, a public low-voltage benchmark network and AC power-flow validation. The main conclusions are:

1. Network-aware control is essential in weak feeders. Uncontrolled charging violated the 0.90 pu voltage limit in 6.4% of charging intervals and overloaded the transformer by up to 35%, whereas all controlled strategies stayed within limits.
2. Outage awareness reduces unmet energy, increasingly so as supply worsens: by 4%, 14% and 22% relative to outage-unaware least-laxity-first at 19, 15 and 12 h of daily supply.
3. A simple outage-aware least-laxity rule performed as well as MPC (cost within 0.2%), at negligible computational cost.
4. PPO agents reduced the daily cost by 1–5% relative to MPC under realistic forecast errors, by rationing generator energy more cautiously. Their advantage depended on the training seed, disappeared when information they had been trained with was missing, and turned into a 22–28% disadvantage when true departure times became available.
5. Departure-time uncertainty, not outage uncertainty, dominates the remaining gap to perfect information (87% of the gap). Collecting departure times from users is the most effective improvement.

Future work should test the controllers with measured outage logs, for example recorded by IoT monitoring nodes [27], and with local charging data from Iraqi distribution networks, extend the comparison to multi-feeder and unbalanced networks, and investigate hybrid RL-MPC schemes that combine the robustness of optimisation with the learned handling of uncertainty.

Funding or Acknowledgment

The author received no external funding for this study. The author thanks the Caltech Adaptive Charging Network for making the ACN-Data charging sessions publicly available and the SimBench project for the public low-voltage benchmark network.

Conflicts of Interest

The author declares no conflicts of interest.

Data Availability

The charging sessions are from the public ACN-Data set (Caltech), and the network and household profiles from the public SimBench data set. The processed data, the simulator, the controllers and the trained agents are available from the corresponding author on reasonable request.

References

[1] S. Powell, G. Vianna Cezar, L. Min, I. M. L. Azevedo, and R. Rajagopal, "Charging infrastructure access and operation to reduce the grid impacts of deep electric vehicle adoption," *Nature Energy*, vol. 7, no. 10, pp. 932–945, 2022, doi: 10.1038/s41560-022-01105-7.

[2] S. Ghanbari Motlagh, J. Oladigbolu, and L. Li, "A review on electric vehicle charging station operation considering market dynamics and grid interaction," *Applied Energy*, vol. 392, Art. no. 126058, 2025, doi: 10.1016/j.apenergy.2025.126058.

[3] D. Qiu, Y. Wang, W. Hua, and G. Strbac, "Reinforcement learning for electric vehicle applications in power systems: A critical review," *Renewable and Sustainable Energy Reviews*, vol. 173, Art. no. 113052, 2023, doi: 10.1016/j.rser.2022.113052.

[4] H. A. Mutar, I. J. Mohammed, and I. R. N. ALRubeei, "AI for solar PV forecasting, MPPT, and energy management: A comprehensive review," *International Journal of Computational and Electronic Aspects in Engineering*, vol. 7, no. 1, pp. 100–114, 2026, doi: 10.26706/ijceae.7.1.20260111.

[5] A. A. Hadi, "The impact of artificial neural network (ANN) on the solar energy cells: A review," *International Journal of Computational and Electronic Aspects in Engineering*, vol. 5, no. 1, pp. 30–41, 2024, doi: 10.26706/ijceae.5.1.20240505.

[6] A. Al-Wakeel, "Local energy systems in Iraq: Neighbourhood diesel generators and solar photovoltaic generation," in *Microgrids and Local Energy Systems*, N. Jenkins, Ed. London, U.K.: IntechOpen, 2021, doi: 10.5772/intechopen.95280.

[7] Z. Ali and H. Athari, "Beyond barrels and generators: Solar power economics and market potential in Iraq," *NTU Journal of Renewable Energy*, vol. 10, no. 1, pp. 31–38, 2026, doi: 10.56286/nkp6b206.

[8] M. Wiese and L.-M. van der Westhuizen, "Impact of planned power outages (load shedding) on consumers in developing countries: Evidence from South Africa," *Energy Policy*, vol. 187, Art. no. 114033, 2024, doi: 10.1016/j.enpol.2024.114033.

[9] G. Yu, X. Ye, and X. Xia, "Optimal parking lot retrofit planning for electric vehicle charging station during prolonged load shedding," *Energy*, vol. 322, Art. no. 135624, 2025, doi: 10.1016/j.energy.2025.135624.

[10] J. Einolander, A. Kiviaho, and R. Lahdelma, "Valuing the household power outage self-sustainment capabilities of bidirectional electric vehicle charging," *Applied Energy*, vol. 374, Art. no. 124071, 2024, doi: 10.1016/j.apenergy.2024.124071.

[11] M. Kadhim, "Improving power quality with active filtering and energy storage technologies in grid-connected hybrid solar-wind renewable energy systems," *International Journal of Computational and Electronic Aspects in Engineering*, vol. 7, no. 2, pp. 291–304, 2026, doi: 10.26706/ijceae.7.2.20260317.

[12] A. Di Giorgio, E. De Santis, L. Frettoni, S. Felli, and F. Liberati, "Electric vehicle fast charging: A congestion-dependent stochastic model predictive control under uncertain reference," *Energies*, vol. 16, no. 3, Art. no. 1348, 2023, doi: 10.3390/en16031348.

[13] B. Kandpal, P. Pareek, and A. Verma, "A robust day-ahead scheduling strategy for EV charging stations in unbalanced distribution grid," *Energy*, vol. 249, Art. no. 123737, 2022, doi: 10.1016/j.energy.2022.123737.

[14] Y. Li, Z. Zhang, and Q. Xing, "Real-time online charging control of electric vehicle charging station based on a multi-agent deep reinforcement learning," *Energy*, vol. 319, Art. no. 135095, 2025, doi: 10.1016/j.energy.2025.135095.

[15] S. H. Mansour, S. M. Azzam, H. M. Hasanien, M. Tostado-Véliz, A. Alkuhayli, and F. Jurado, "Deep reinforcement learning-based plug-in electric vehicle charging/discharging scheduling in a home energy management system," *Energy*, vol. 316, Art. no. 134420, 2025, doi: 10.1016/j.energy.2025.134420.

[16] S. Zhang, R. Jia, H. Pan, and Y. Cao, "A safe reinforcement learning-based charging strategy for electric vehicles in residential microgrid," *Applied Energy*, vol. 348, Art. no. 121490, 2023, doi: 10.1016/j.apenergy.2023.121490.

[17] D. Liu, P. Zeng, S. Cui, and C. Song, "Deep reinforcement learning for charging scheduling of electric vehicles considering distribution network voltage stability," *Sensors*, vol. 23, no. 3, Art. no. 1618, 2023, doi: 10.3390/s23031618.

[18] J. Arroyo, C. Manna, F. Spiessens, and L. Helsen, "Reinforced model predictive control (RL-MPC) for building energy management," *Applied Energy*, vol. 309, Art. no. 118346, 2022, doi: 10.1016/j.apenergy.2021.118346.

[19] Z. J. Lee, T. Li, and S. H. Low, "ACN-Data: Analysis and applications of an open EV charging dataset," in *Proc. 10th ACM Int. Conf. Future Energy Systems (e-Energy '19)*, 2019, pp. 139–149, doi: 10.1145/3307772.3328313.

[20] S. Meinecke, D. Sarajlić, S. R. Drauz, et al., "SimBench—A benchmark dataset of electric power systems to compare innovative solutions based on power flow analysis," *Energies*, vol. 13, no. 12, Art. no. 3290, 2020, doi: 10.3390/en13123290.

[21] N. Chen, C. Kurniawan, Y. Nakahira, L. Chen, and S. H. Low, "Smoothed least-laxity-first algorithm for electric vehicle charging: Online decision and performance analysis with resource augmentation," *IEEE Transactions on Smart Grid*, vol. 13, no. 3, pp. 2209–2217, 2022, doi: 10.1109/TSG.2021.3138615.

[22] L. Thurner, A. Scheidler, F. Schäfer, et al., "pandapower—An open-source Python tool for convenient modeling, analysis, and optimization of electric power systems," *IEEE Transactions on Power Systems*, vol. 33, no. 6, pp. 6510–6521, 2018, doi: 10.1109/TPWRS.2018.2829021.

[23] *Voltage Characteristics of Electricity Supplied by Public Electricity Networks*, EN 50160, European Committee for Electrotechnical Standardization (CENELEC), Brussels, Belgium, 2010.

[24] Q. Huangfu and J. A. J. Hall, "Parallelizing the dual revised simplex method," *Mathematical Programming Computation*, vol. 10, no. 1, pp. 119–142, 2018, doi: 10.1007/s12532-017-0130-5.

[25] J. Schulman, F. Wolski, P. Dhariwal, A. Radford, and O. Klimov, "Proximal policy optimization algorithms," arXiv:1707.06347, 2017, doi: 10.48550/arXiv.1707.06347.

[26] A. Raffin, A. Hill, A. Gleave, A. Kanervisto, M. Ernestus, and N. Dormann, "Stable-Baselines3: Reliable reinforcement learning implementations," *Journal of Machine Learning Research*, vol. 22, no. 268, pp. 1–8, 2021. Available online: https://jmlr.org/papers/v22/20-1364.html

[27] O. A. Abdaumran, "IoT-enabled real-time fault monitoring in overhead power lines using ESP32 and Arduino integrated development," *International Journal of Computational and Electronic Aspects in Engineering*, vol. 6, no. 3, pp. 190–201, 2025, doi: 10.26706/ijceae.6.3.20250610.

[28] I. A. Ameen and M. A. Al-Sheikh, "Wireless sensor networks for smart gardening: ESP-NOW and Blynk IoT integration for water and energy optimization," *International Journal of Computational and Electronic Aspects in Engineering*, vol. 5, no. 3, pp. 101–115, 2024, doi: 10.26706/ijceae.5.3.20240804.

[29] S. Waghe, U. Kuradkar, S. Prajapati, and R. Mohane, "Detecting and reducing phantom power: A human-centric IoT approach," *International Journal of Computational and Electronic Aspects in Engineering*, vol. 7, no. 3, pp. 76–83, 2026, doi: 10.26706/ijceae.7.3.20260711.

[30] A. W. Talab, "Improving communication protocols based on crucial data transmission security for IoT techniques," *International Journal of Computational and Electronic Aspects in Engineering*, vol. 6, no. 1, pp. 1–11, 2025, doi: 10.26706/ijceae.6.1.20250203.

[31] S. Q. Ameen, R. G. S. Alsulta, Z. S. Hussain, and Z. T. Abdul-Rahmman, "A hybrid RSA–ElGamal framework for secure end-to-end communications in resource-constrained IoT networks," *International Journal of Computational and Electronic Aspects in Engineering*, vol. 7, no. 2, pp. 140–153, 2026, doi: 10.26706/ijceae.7.2.20260303.